

Supporting Information

Absolute determination of the chemical kinetic rate constant by optical tracking the reaction on the second timescale using cavity-enhanced absorption spectroscopy

Hongming Yi^{1*}, Lingshuo Meng^{1,2}, Tao Wu^{3#}, Amélie Lauraguais¹, Cecile Coeur¹, Alexandre Tomas², Hongbo Fu⁴, Xiaoming Gao⁵, Weidong Chen^{1#}

¹ *Laboratoire de Physicochimie de l'Atmosphère, Université du Littoral Côte d'Opale, 59140 Dunkerque, France*

² *IMT Nord Europe, Institut Mines-Télécom, Univ. Lille, Center for Energy and Environment, 59000 Lille, France*

³ *Key Laboratory of Nondestructive Test, Nanchang Hangkong University, Nanchang 330063, China*

⁴ *Shanghai Key Laboratory of Atmospheric Particle Pollution and Prevention, Institute of Atmospheric Sciences, Fudan University, Shanghai, 200433, China*

⁵ *Anhui Institute of Optics and Fine Mechanics, Chinese Academy of Sciences, Hefei 230031, China*

* *now with Department of Civil and Environmental Engineering, Princeton University, Princeton, NJ 08544, USA*

Corresponding Authors: Weidong Chen (chen@univ-littoral.fr); Tao Wu (wutccnu@nchu.edu.cn)

Contents:

Optical instrument description: Performance characterization of the developed optical instruments-----S2

List of Figures:

Figure S1. Picture of the LED-IBBCEAS and EC-QCL MPC setups installed in the atmospheric simulation chamber for simultaneous measurements of NO₃, NO₂ and N₂O₅ concentrations-----S3

Figure S2. NO₂ and NO₃ absorption cross sections, mirror reflectivity and LED emission spectrum in the wavelength range 610 - 690 nm-----S4

Figure S3. Comparison between the NO₂ concentrations measured by LED-IBBCEAS and chemiluminescence NO_x analyzer without interferences (i.e., before ozone introduction; 0-1200 s in Figure 4(a))-----S4

Figure S4. Broadband absorption spectra of 257 ppbv NO₂ and 1.683 ppbv NO₃ in association with the corresponding fit spectra-----S5

Figure S5. Measured (in 25 s) and fitted EC-QCL MPC direct absorption spectra of 30 ppbv N_2O_5 from 1223 to 1263 cm^{-1} associated with residual for detection limit evaluation-----S6

Figure S6. Allan deviation for evaluation of the performances of the developed (a) LED-IBBCEAS and (b) EC-QCL MPC apparatus-----S7

Figure S7. Frequency distribution of zero- NO_3 , zero- NO_2 , zero- N_2O_5 and zero- O_3 mixing ratios measured by IBBCEAS, EC-QCL MPC and photometric analyzer with integration time of 25 s, respectively-----S8

List of Tables:

Tables S1-S3. Summarized rate constants between NO_3 and VOCs (propanal, isoprene, formaldehyde) measured by different techniques from the literature values-----S9

References-----S10

Performance characterization of the developed optical instruments

The developed LED-IBBCEAS and EC-QCL MPC setups (as shown in Figure S1) were evaluated by simultaneous optical tracing of NO_3 , NO_2 and N_2O_5 concentrations. First, NO_2 with concentrations varying from 100 ppbv (part per billion by volume) to 2 ppmv (part per million by volume) was injected into the simulation chamber. The corresponding NO_2 concentrations measured by a Thermo 42i NO_x analyzer were used to determine the cavity mirror reflectivity $R(\lambda)$ (Figure S2), as described in [1]. The reference absorption cross-sections (in $[\text{cm}^2 \cdot \text{molecule}^{-1}]$) of NO_2 [2] and NO_3 [3] (Figure S2) used for concentration retrievals, associated with the LED emission spectrum, are also given in Figure S2. Approximately 1.1 ppmv of O_3 generated from a corona discharge ozone generator (C-L010-DTI, C-Lasky) was introduced into the chamber after a prior injection of 2 ppm NO_2 to produce NO_3 . In the presence of an excess of NO_2 , the NO_3 reaction with NO_2 to produce N_2O_5 also occurs once NO_3 is formed. Time-series measurements of NO_2 , NO_3 and N_2O_5 concentrations were simultaneously performed using the LED-IBBCEAS and EC-QCL MPC instruments. Typical broadband absorption spectra of NO_3 , NO_2 , N_2O_5 and the corresponding fits for their concentration retrievals are given in Figures S3 and S4. Figure S3(a) shows LED-IBBCEAS-based simultaneous measurement of broadband absorption spectra of ~ 1.7 ppbv NO_3 and ~ 260 ppbv NO_2 . Figure S3(b) presents the decomposed fitted absorption spectrum of each species. $1-\sigma$ detection limits (DL) of 2.2 (1.0) pptv for NO_3 and 1.6 (0.8) ppbv for NO_2 in 25 s (120 s) integration time were deduced based on the fit residual shown in Figure S3(c). EC-QCL MPC measurement of ~ 30 ppbv N_2O_5 absorption and the corresponding fit residual are given in Figures S4(a) and S4(b), respectively. The corresponding DL for N_2O_5 was ~ 12 (2.6) ppbv in a 25 (600) s integration time. Using the estimation methods given in [1] for NO_2 and NO_3 and in [4] for N_2O_5 , the overall uncertainties in the retrieved concentrations are 9.1% for NO_2 , 11% for NO_3 , $\sim 10\%$ for N_2O_5 , and 3.2% for O_3 measured with an O_3 photometric analyzer.

Allan variance analysis [4-5] was carried out to determine the optimum integration time and the corresponding DL, and the results are shown in Figures S5(a, b). The system stabilization times for the LED-IBBCEAS and the EC-QCL MPC apparatus were approximately 500 s and 600 s, respectively, which resulted in DLs of 0.4 pptv for NO₃, 0.4 ppbv for NO₂ and 2.1 ppbv for N₂O₅. Although a higher DL could be obtained with longer integration times of 500 s for NO₃ and 600 s for N₂O₅, a 25 s integration time is a good compromise between DL and the time response required to measure real-time concentrations of N₂O₅ in our study.

In the present work, the measurement precision and DL at an integration time of 25 s were investigated by measuring residual NO₃, NO₂, N₂O₅ and O₃ mixing, which is similar with the method reported in [6]. All measurements were committed to a clean chamber after flushing with synthetic clean air overnight (“zero air” data). In Figures S6(a-d), the frequency distributions of zero-NO₃, zero-NO₂, zero-N₂O₅ and zero-O₃ measurements are shown. A Gaussian distribution was fitted to the histograms to visualize the mean of the zero measurements and their standard deviation (the measure of the actual instrumental measurement precision). Measurement precisions of 1.8 pptv, 1.8 ppbv, 11.7 ppbv and 0.3 ppbv were found for NO₃, NO₂, N₂O₅, and O₃, respectively. The calculated mean NO₃, NO₂ and N₂O₅ mixing ratios are very close to the deduced DL from the spectral fit in Figs. 2 and 3. The fitted mean O₃ mixing ratios deviate no more than ± 0.2 ppbv from zero.

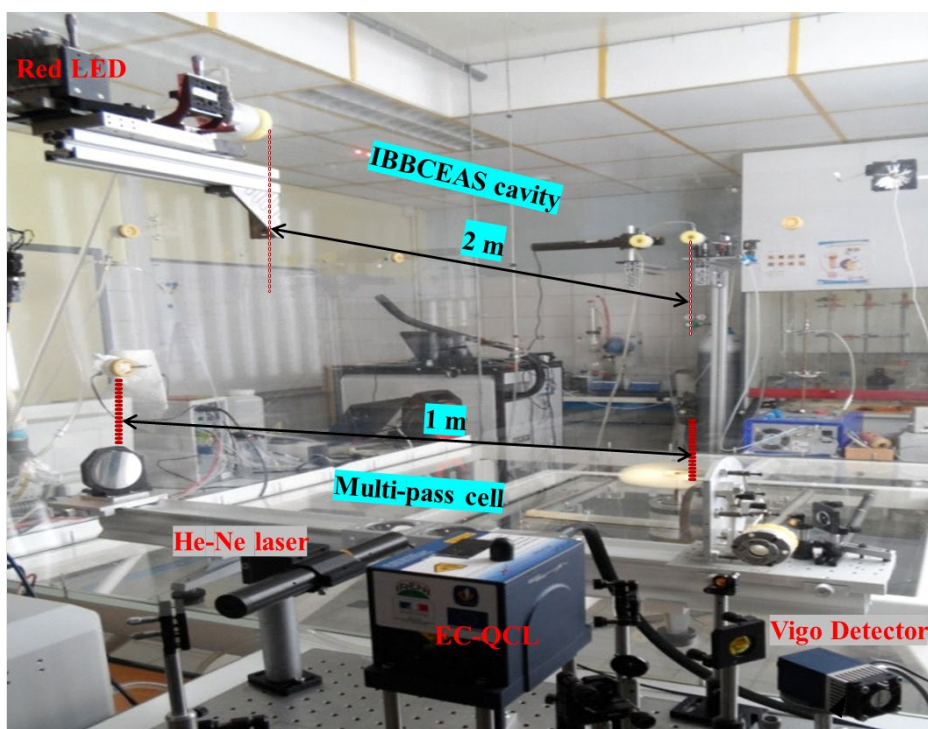


Figure S1. Picture of the LED-IBBCEAS and EC-QCL MPC setups installed in the present atmospheric simulation chamber for simultaneous measurements of NO₃, NO₂ and N₂O₅ concentrations.

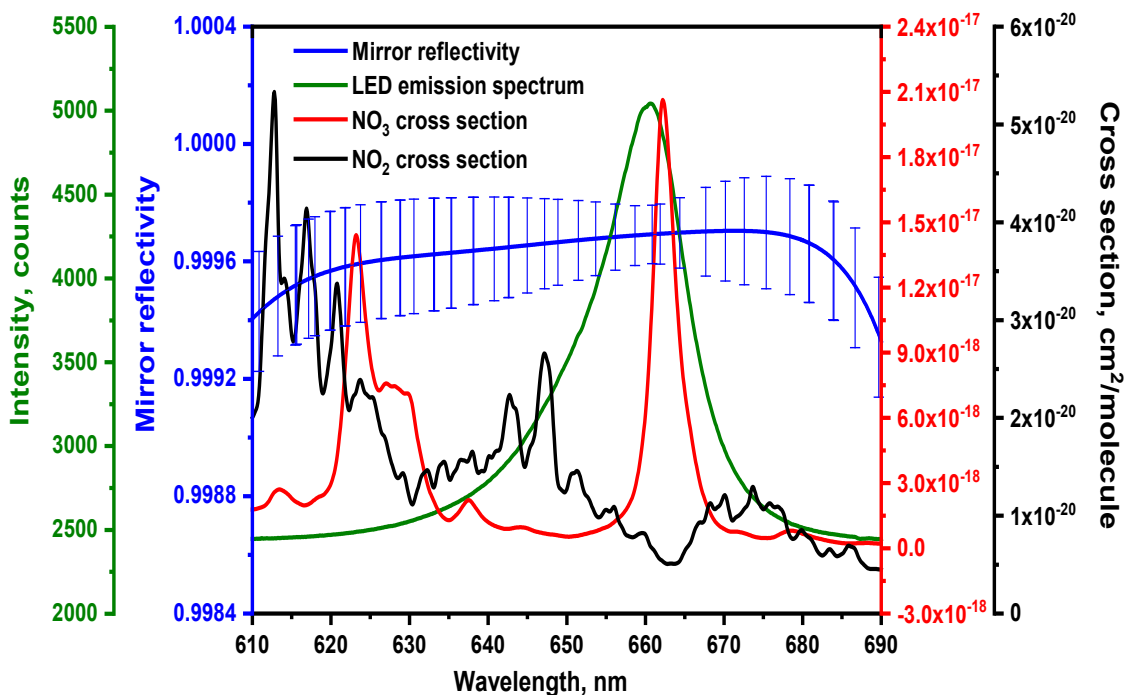


Figure S2. NO₂ and NO₃ absorption cross sections, mirror reflectivity and LED emission spectrum in the wavelength range 610 - 690 nm.

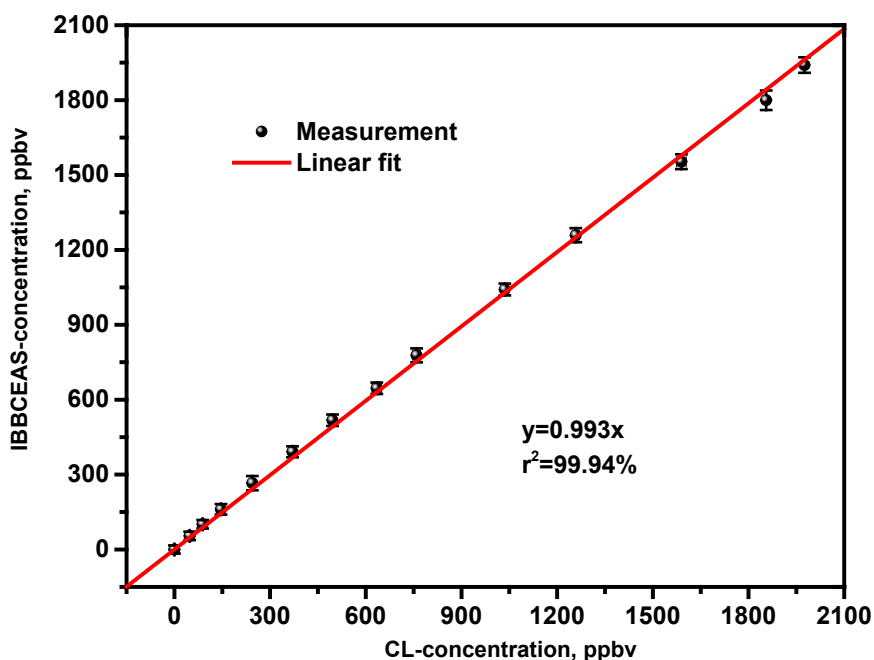


Figure S3. Comparison between the NO₂ concentrations measured by LED-IBBCEAS and chemiluminescence (CL) NO_x analyzer without interferences (i.e., before ozone introduction; 0-1200 s in Fig. 2(a)).

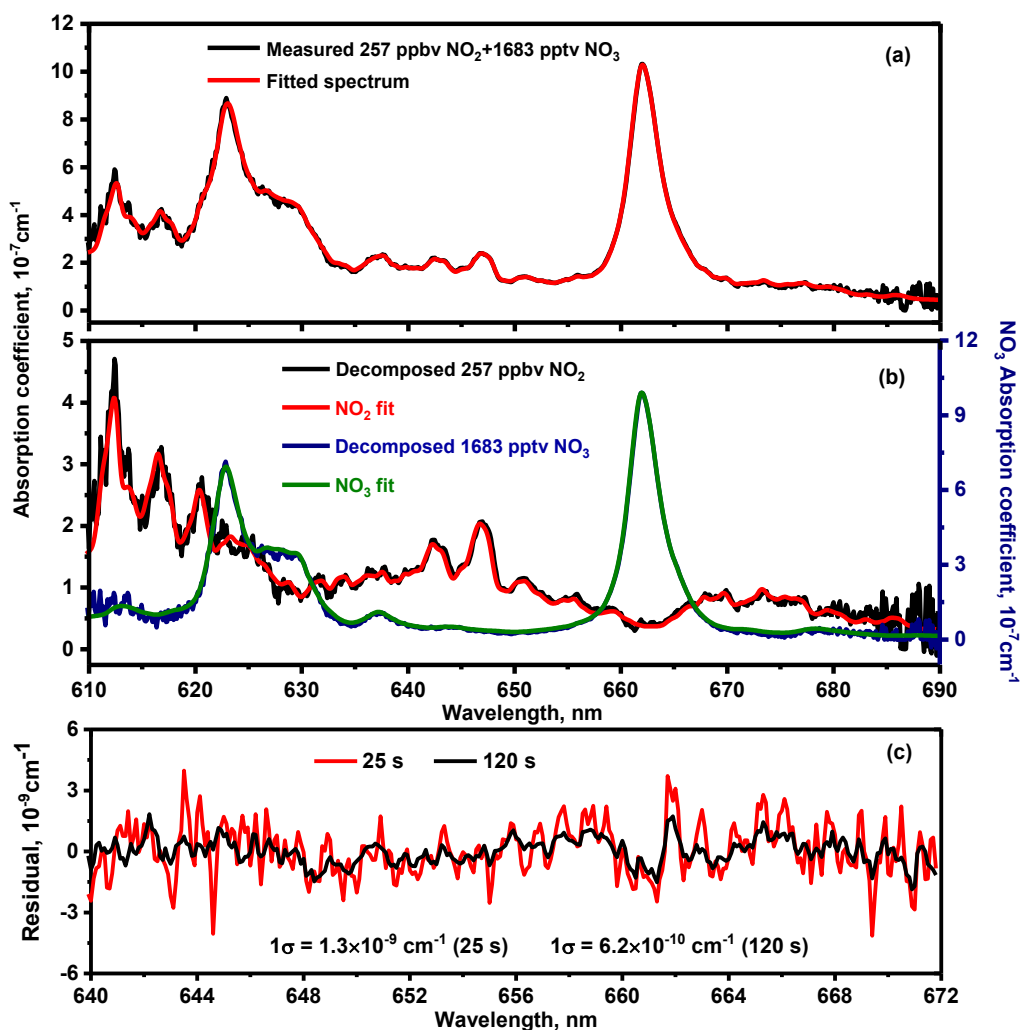


Figure S4. Broadband absorption spectra of 257 ppbv NO_2 and 1.683 ppbv NO_3 in association with the corresponding fit spectra: (a) Recorded IBBCEAS spectrum (black) and its fit (red) leading to 257 ppbv NO_2 and 1.683 ppbv NO_3 ; (b) The corresponding decomposed spectra; (c) The fit residual in the spectral region of 640-672 nm (chosen for simultaneous measurement of NO_2 and NO_3), used for evaluation of detection limits.

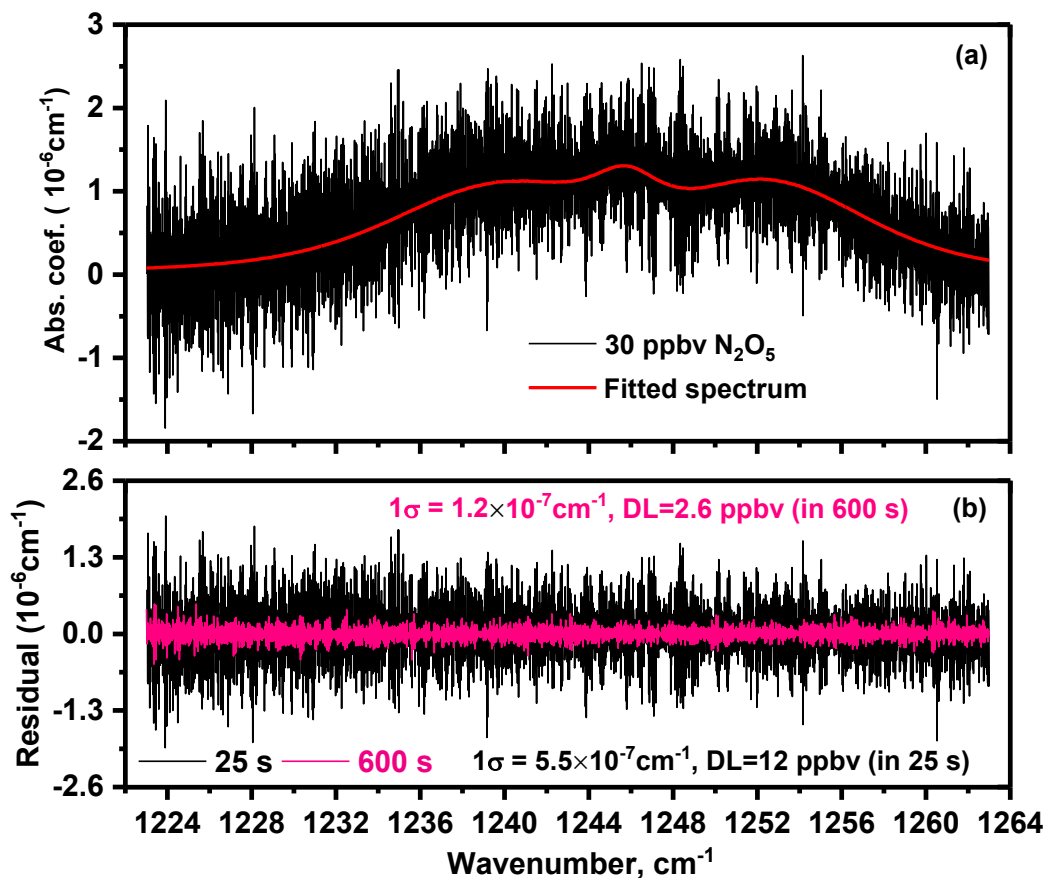


Figure S5. (a): Measured (in 25 s) and fitted EC-QCL MPC direct absorption spectra of 30 ppbv N_2O_5 from 1223 to 1263 cm^{-1} . (b): Fit residual with 25 s and 600 s integration time (used for estimation of detection limit).

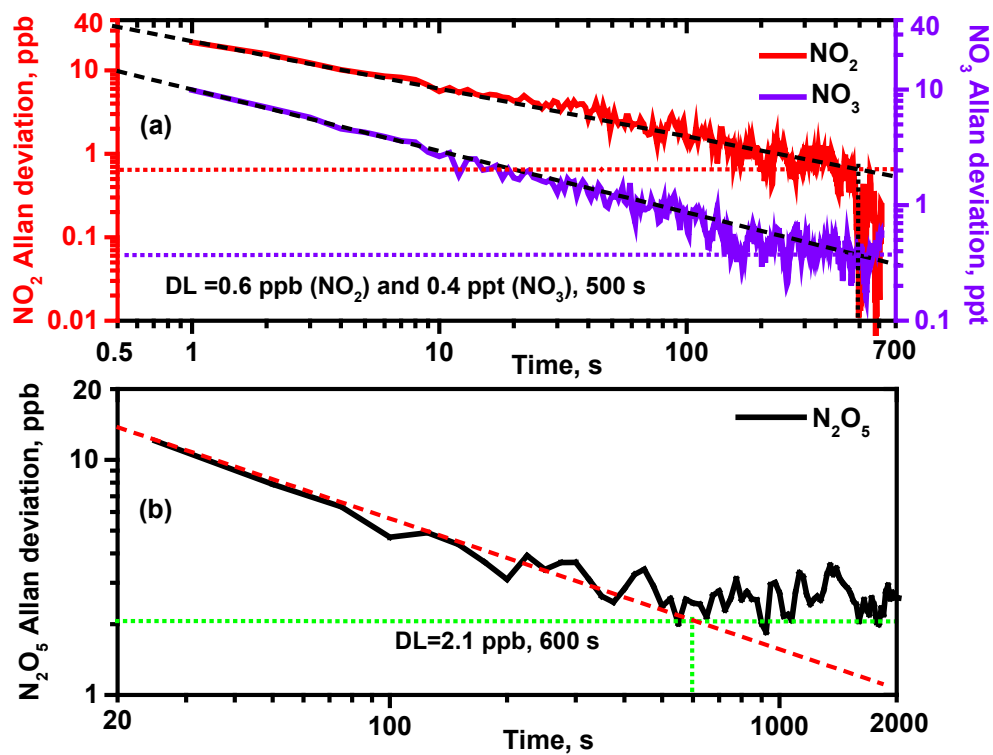


Figure S6. Allan deviation for performance evaluation of the developed (a) LED-IBBCEAS and (b) EC-QCL MPC apparatus.

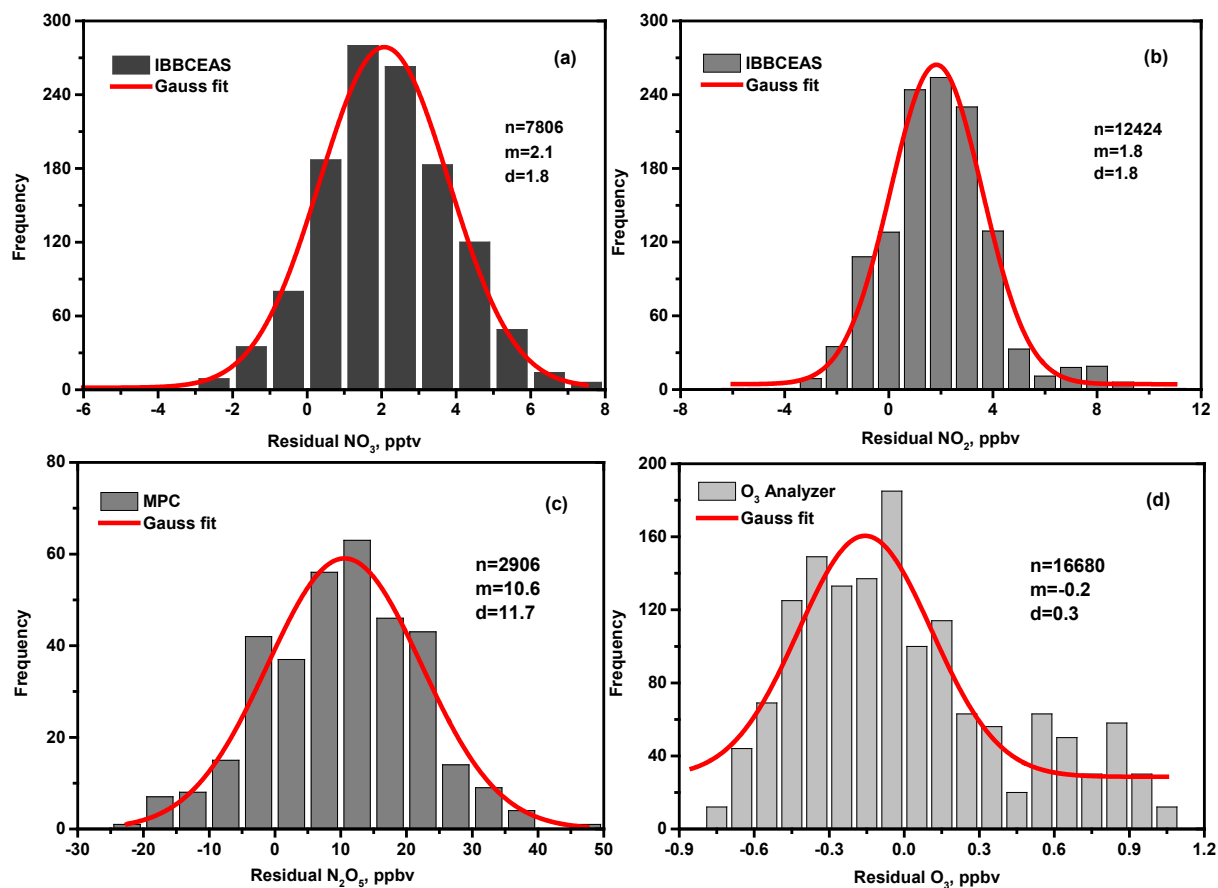


Figure S7. Frequency distribution of zero- NO_3 , zero- NO_2 , zero- N_2O_5 and zero- O_3 mixing ratios measured by IBBCEAS, EC-QCL MPC and photometric analyzer with an integration time of 25 s. A normal distribution (red line) was fitted to the histograms. n is the number of statistically available data points; the 1σ standard deviation, d is a measure of the instrumental precision; m denotes the mean retrieved NO_3 , NO_2 , N_2O_5 and O_3 mixing ratios (standardizing for the detection limit) from zero air spectra.

Table S1. Rate constants ($k_{\text{C}_3\text{H}_6\text{O}}$ in $10^{-15} \text{ cm}^3 \text{ molecule}^{-1} \text{ s}^{-1}$) for the reaction of NO_3 with propanal ($\text{C}_3\text{H}_6\text{O}$) determined at $293 \pm 2 \text{ K}$ and atmospheric pressure and literature data for comparison.

Ref. No. (m)	$k_{\text{C}_3\text{H}_6\text{O}}$	Temperature (K)	Measurement technique ^a	References*
3	8.94±6.18	298	Eq. calculation	[7] (Cabañas et al., 2001)
4	6.0±0.6	298±2	AR (DF-LIF)	
5	5.8±1.0	300±3	AR (DOAS and GC)	[8] (Bossmeier et al., 2006)
6	5.80±0.48	298±2	RR	[7] (D'Anna and Nielsen, et al., 1997)
7	7.28±0.41	296±2	RR	[7] (Papagni et al., 2000)
8	6.18±0.57	298±2	RR	[7] (D'Anna et al., 2001)

^aDF-LIF: Discharge flow tube reactor with laser-induced fluorescence; DOAS: Differential Optical Absorption Spectroscopy GC: dual-column gas-chromatograph with cryo-focus module and two flame ionization detectors RR-relative rate method; AR.: Absolute Rate method. Here, [7] stands for the citation from page 3804 of review reference 7.

Table S2. Rate constants ($k_{\text{C}_5\text{H}_8}$ in $10^{-13} \text{ cm}^3 \text{ molecule}^{-1} \text{ s}^{-1}$) for reactions of NO_3 with isoprene (C_5H_8), determined at $293 \pm 2 \text{ K}$ and atmospheric pressure, and literature data.

Ref. No. (m)	$k_{\text{C}_5\text{H}_8}$	Temperature (K)	Measurement technique ^a	References
3	13.0±1.4	298	AR (DF-MS)	[7] (Benter and Schindler, 1988)
4	6.69±1.59	298	Eq. calculation	[7] (Dlugokencky and Howard, 1989)
5	6.52±0.31	293	AR (F-LIF)	
6	7.30±0.44	298	AR (DF-MS)	[7] (Wille et al., 1991)
7	8.26±0.60	298	AR (DF-MS)	[7] (Wille et al., 1991; Lancar et al., 1991)
8	10.7±2.0	295±2	AR (PR-A)	[7] (Ellermann et al., 1992)
9	7.3±0.2	298±2	AR (F-CIMS)	[7] (Suh et al., 1992)
10	5.94±0.16	295±1	RR	[7] (Atkinson et al., 1984)
11	12.1±2.0	298±2	RR	[7] (Barnes et al., 1990)
12	6.86±0.55	298	RR	[7] (Berndt and Böge, 1997)
13	5.33±0.21	296±2	RR	[7] (Stabel et al., 2004)
14	7.0±0.6	296±2	RR	
15	6.13±0.12	295±2	RR	[7] (Zhao et al., 2011)

^aDF-MS: Discharge flow-mass spectrometer; PR-A: pulse radiolysis combined with kinetic ultraviolet visible absorption spectroscopy; F-LIF: Flow tube reactor with laser-induced fluorescence; F-CIMS: Fast-flow reactor coupled to chemical ionization mass spectrometry. RR-Relative Rate method; AR: Absolute Rate method. Here, [7] stands for the citation from page 3796 of review reference 7.

Table S3. Rate constant ($k_{\text{CH}_2\text{O}}$ in $10^{-16} \text{ cm}^3 \text{ molecule}^{-1} \text{ s}^{-1}$) for reactions between NO_3 and formaldehyde (CH_2O) determined at $293 \pm 2 \text{ K}$ and atmospheric pressure and literature data.

Ref. No. (m)	$k_{\text{CH}_2\text{O}}$	Temperature (K)	Measurement technique	References
3	5.8 ± 0.4	300 ± 1	(AR) N_2O_5 decay-FTIR ^a	[7] (Cantrell et al., 1985)
4	5.2 ± 0.9	298 ± 2	(AR) NO_3 absorption-FTIR	[7] (Doussin et al., 2003)
5	4.75 ± 0.39	298 ± 1	RR	[9] (Atkinson et al., 1984c)
6	7.2 ± 1.1	298 ± 2	RR	[7] Cantrell et al., 1985
7	11.5 ± 2.4	295 ± 2	RR	[7] (Hjorth, 1988)

^aFTIR: Fourier transform infrared spectroscopy; AR: absolute rate method; RR-relative rate method. Here, [7] stands for the citation from page 3800 of review reference 7.

References

1. T. Wu, C. Coeur-Tourneur, G. Dhont, A. Cassez, E.; Fertein, X. He and W. Chen, Application of IBBCEAS to kinetic study of NO_3 radical formation from $\text{O}_3 + \text{NO}_2$ reaction in an atmospheric simulation chamber, *J. Quant. Spectrosc. Rad. Transfer*, 2014, **133**, 199–205.
2. S. Voigt, J. Orphal and J. P. Burrows, The temperature and pressure dependence of the absorption cross-sections of NO_2 in the 250-800 nm region measured by Fourier transform spectroscopy, *J. Photochem. Photobiol. A: Chem.*, 2002, **149**, 1-7.
3. J. Orphal, C. E. Fellows and P.-M. Flaud, The visible absorption spectrum of NO_3 measured by high-resolution Fourier transform spectroscopy, *J. Geophys. Res.*, 2003, **108**, D3, 4077.
4. H. Yi, T. Wu, A. Lauraguais, V. Semenov, C. Coeur, A. Cassez, E. Fertein, X. Gao and W. Chen, High accuracy and high-sensitivity spectroscopic measurement of dinitrogen pentoxide (N_2O_5) in an atmospheric simulation chamber using a quantum cascade laser, *Analyst*, 2017, **142**, 4638–4646.
5. H. Yi, T. Wu, G. Wang, W. Zhao, E. Fertein, C. Coeur, X. Gao, W. Zhang and W. Chen, Sensing atmospheric reactive species using light emitting diode by incoherent broadband cavity enhanced absorption spectroscopy, *Opt. Express*, 2016, **24**, A781-A790.
6. H.-P. Dorn, R. L. Apodaca, S. M. Ball, T. Brauers, S. S. Brown, J. N. Crowley, W. P. Dubé, H. Fuchs, R. Häseler, U. Heitmann, R. L. Jones, A. Kiendler-Scharr, I. Labazan, J. M. Langridge, J. Meinen, T. F. Mentel, U. Platt, D. Pöhler, F. Rohrer, A. A. Ruth, E. Schlosser, G. Schuster, A. J. L. Shillings, W. R. Simpson, J. Thieser, R. Tillmann, R. Varma, D. S. Venables and A. Wahner, Intercomparison of NO_3 radical detection instruments in the atmosphere simulation chamber SAPHIR, *Atmos. Meas. Tech.*, 2013, **6**, 1111-1140.
7. R. Atkinson, D. L. Baulch, R. A. Cox, J. N. Crowley, R. F. Hampson, R. G. Hynes, M. E. Jenkin, M. J. Rossi and J. Troe, Evaluated kinetic and photochemical data for atmospheric chemistry: Volume II-gas phase reactions of organic species, *Atmos. Chem. Phys.*, 2006, **6**, 3625–4055.
8. J. Bossmeyer, T. Brauers, C. Richter, F. Rohrer, R. Wegener and A. Wahner, Simulation chamber studies on the NO_3 chemistry of atmospheric aldehydes, *Geophys. Res. Lett.*, 2006, **33**, L18810, doi:10.1029/2006GL026778.
9. R. Atkinson, C. N. Plum, W. P. L. Carter, A. M. Winer and J. N., Jr. Pitts, Rate constants for the gas-phase reactions of nitrate radicals with a series of organics in air at $298 \pm 1 \text{ K}$, *J. Phys. Chem.*, 1984, **88**, 1210-1215.